2. Long-range and other corrections for density functionals

2.1. Conventional correction schemes in density functional theory

In this century, the main concerns of theoretical chemistry obviously make the transition from accurate investigations of small molecules to the designs of complicated large molecular systems; *e.g.* proteins, nano-materials, environmental catalyses, and so forth. What is necessary for approaching these systems is an accurate theory of low computational order. Density Functional Theory (DFT)[1,2,3] is expected to be a major candidate for such a theory at present, because this theory gives accurate chemical properties despite of its low computational order that may be reduced to order-*N*. In DFT, electronic states are usually determined by solving the nonlinear Kohn-Sham equation[1] with an exchange-correlation density functional. The most remarkable characteristic of DFT is the exchange-correlation energy part that is approximated by a one-electron potential functional. Hence, calculated DFT results depend on the form of this exchange-correlation functional.

In last two decades, various kinds of exchange functionals have been suggested especially for generalized gradient approximations (GGA)[4,5,6,7] beyond the local density approximation (LDA) functional.[8] Due to the requirement of order, these GGA exchange functionals are usually expressed as a functional of $x_\sigma = |\nabla\rho_\sigma| / \rho_\sigma^{4/3}$, where ρ_σ is the electron density of spin σ and $\nabla\rho_\sigma$ is the gradient of the density.[9] What should be noticed is that most GGA exchange functionals have unique behaviors only for large x_σ.[9,10] This is because small-x_σ behaviors of functionals are restricted by the physical condition for slowly-varying density,[11] although there is no definite conditions for rapidly-varying density.[7,9,10] Hence, GGA exchange functionals are usually characterized by the behaviors for large-x_σ (*i.e.* low-density-high-gradient) density. Conventional exchange-correlation functionals will be discussed by Prof. Scuseria in this book. We will give a summary account of correction schemes for exchange functionals in this section.

Since the latter half of 1990s, hybrid functionals have appeared in DFT calculations. In hybrid functionals, (pure) GGA functionals are combined with the Hartree-Fock (HF) exchange integral at a constant rate. This idea may have come from an observation that DFT calculations using pure GGA functionals often give opposite errors to those in HF calculations. In 1993, Becke suggested hybrid B3LYP functional.[12] Based on a concept of adiabatic connection, B3LYP exchange-correlation energy are expressed by a combination of Becke 1988 (B88) exchange[4] and Lee-Yang-Parr (LYP) correlation[13] GGA functionals, Slater (S) exchange[8] and Vosko-Wilk-Nusair (VWN) correlation[14] LDA functionals, and the HF exchange integral with 3 parameters:

$$E_{xc}^{B3LYP} = a_0 E_x^{HF} + (1-a_0)E_x^S + a_x E_x^{B88} + (1-a_c)E_c^{VWN} + a_c E_c^{LYP}, \quad \textbf{(1)}$$

where E_x^A and E_c^B are exchange and correlation energies of A and B, and a_0, a_x, and a_c are 0.2, 0.72, and 0.81, respectively. Atomic units have been used ($\hbar = e^2 = m = 1$, energies are in hartree, and distances are in bohr). This adiabatic connection may have some incompatible parts; for example, parameters in B88 and LYP functionals were originally determined to reproduce exact exchange and correlation energies. Nevertheless, B3LYP becomes the most popular DFT functional in quantum chemisty, because it gives very accurate results for a wide variety of chemical properties. Becke 1997 (B97)[15] and Perdew-Burke-Ernzerhof 1996 (PBE0)[16] functionals are also hybrid functionals. Similarly to B3LYP, these functionals combine GGA functionals with the HF exchange integral at a constant rate, and give accurate results for various chemical properties of molecules. However, inconsistencies in the adiabatic connection remains unsettled in these functionals.

Asymptotic corrections for exchange functionals have attracted attentions especially in time-dependent DFT (TDDFT) studies. In far regions from atomic nuclei, it is proved that exchange potential for σ-spin electrons, $v_{xc}^{\sigma} = \delta E_{xc} / \delta \rho_{\sigma}$ has the asymptotic relation,[17]

$$\lim_{R\to\infty} v_{xc}^{\sigma}(\mathbf{R}) = -\frac{1}{R}, \quad \textbf{(2)}$$

where R = $|\mathbf{R}|$ and $\mathbf{R}$ is the distance vector from the nearest nucleus. On the ground of this relation, Van Leeuwen and Baerends suggested an exchange functional (LB)[18] by adapting the B88 exchange functional to the asymptotic behavior. Tozer and Handy suggested the asymptotic correction (AC) scheme that imposes, instead of Eq. (**2**),[19,20]

$$\lim_{R\to\infty} v_{xc}^{\sigma}(\mathbf{R}) = -\frac{1}{R} + \varepsilon_{\sigma}^{HOMO} + I_{\sigma} \quad \textbf{(3)}$$

where $\varepsilon_{\sigma}^{HOMO}$ is the eigenvalue of the highest occupied σ-spin molecular orbital and I_{σ} is the ionization potential of the σ-spin electron. It has been reported that underestimations of Rydberg excitation energies in TDDFT calculations are modified by using LB and AC schemes.

Besides, self-interaction correction (SIC) is one of the most popular correction schemes. Perdew and Zunger suggested a scheme for the application of SIC to occupied orbitals where the self-interaction components of the Coulomb and exchange energies are simply subtracted from the total exchange-correlation energy,[21]

$$E_{xc}^{SIC}[\rho_{\alpha},\rho_{\beta}] = E_{xc}[\rho_{\alpha},\rho_{\beta}] - \sum_{i,\sigma}\left(\frac{1}{2}\int\frac{\rho_{i\sigma}(\mathbf{R})\rho_{i\sigma}(\mathbf{R}')}{|\mathbf{R}-\mathbf{R}'|}d^3\mathbf{R}d^3\mathbf{R}' + E_{xc}[\rho_{i\sigma},0]\right) \quad \textbf{(4)}$$

and potential,

$$v_{xc}^{i\sigma,SIC}(\mathbf{R}) = \frac{\delta E_{xc}^{SIC}}{\delta \rho_{i\sigma}(\mathbf{R})} = \frac{\delta E_{xc}[\rho_\alpha, \rho_\beta]}{\delta \rho_{i\sigma}(\mathbf{R})} - \int \frac{\rho_{i\sigma}(\mathbf{R}')}{|\mathbf{R}-\mathbf{R}'|} d^3\mathbf{R}' - \frac{\delta E_{xc}[\rho_{i\sigma}, 0]}{\delta \rho_{i\sigma}(\mathbf{R})}, \qquad (5)$$

where $\rho_{i\sigma}$ is the *i*-th orbital component of ρ_σ. This SIC scheme has been frequently used in energy band calculations of solid states for improving underestimated band gap energies. However, this scheme essentially requires an orbital-localization process[22] or transformation of functionals to an orbital-dependent form[23] due to the degrees of freedom in unitary transformations of orbitals. Tsuneda, Kamiya, and Hirao suggested a regional self-interaction correction (RSIC) scheme as a simple SIC method requiring no additional processes.[24] On the ground that total kinetic energy density, $\tau_\sigma^{total} = \sum_i^{occ} |\nabla \psi_{i\sigma}|^2$, approaches the Weizsäcker kinetic energy density, $\tau_\sigma^W = |\nabla \rho_\sigma|^2 / (4\rho_\sigma)$ for self-interacted electrons, an exchange functional is spatially replaced with a self-interaction energy density only for regions, where τ_σ^{total} approaches τ_σ^W, in this scheme. As the self-interaction energy density, exact exchange self-interaction energy densities of 1*s* orbitals in hydrogen-like atoms, $\psi_{i\sigma}^{1s} = \sqrt{\alpha^3/\pi}\exp(-\alpha R)$, is employed such as

$$\varepsilon_{x\sigma}^{RSIC} = -\left(\frac{\rho_\sigma}{2R}\right)\left[1-(1+\alpha R)\exp(-2\alpha R)\right], \qquad (6)$$

where $\varepsilon_{x\sigma}$ is defined by $E_x \equiv \sum_\sigma \int \varepsilon_{x\sigma} d^3\mathbf{R}$ and $\alpha = \nabla\rho_\sigma / (2\rho_\sigma)$. By applying the RSIC scheme to chemical reaction calculations, it was found that underestimated barrier energies of pure functionals were clearly improved for some reactions.

As mentioned above, various correction schemes have been developed up to the present. However, there is room for further improvement in conventional correction schemes; Conventional hybrid functionals give poor excitation energies in TDDFT calculations as mentioned later. Asymptotic and self-interaction corrections have little (or worse) effect on reproducibilities of molecular chemical properties. Recently, it has been proved that a long-range correction for exchange functionals obviously brings solutions to various DFT problems that have never been solved by other functionals or corrections. In later sections, we will briefly review the background of the long-range correction scheme and will reveal the applicabilities of this scheme.

2.2. Long-range correction schemes for exchange functionals

Pure DFT exchange-correlation functionals have been represented by using only local quantities at a reference point: *e.g.* electron density, gradient of density, and etc. (We are now describing ``local'' quantity as a quantity determined at a reference point for clarity, although gradient of density is known as a ``nonlocal" quantity in common use.) It is, therefore, presumed that pure functionals overestimate local contributions and underestimate nonlocal contributions. The most significant nonlocal contribution neglected in pure functionals may be the long-range electron-electron exchange interaction, because it may be impossible to represent this interaction as a functional of a one-electron quantity.

In 1996, Savin suggested a long-range exchange correction scheme for LDA functional.[25] In this scheme, the two-electron operator, $1/r_{12}$, is separated into the short-range and long-range parts naturally by using the standard error function *erf* such that

$$\frac{1}{r_{12}} = \frac{1-erf(\mu r_{12})}{r_{12}} + \frac{erf(\mu r_{12})}{r_{12}}, \tag{7}$$

where $r_{12} = |\mathbf{r_1} - \mathbf{r_2}|$ for coordinate vectors of electrons, $\mathbf{r_1}$ and $\mathbf{r_2}$, and μ is a parameter that determines the ratio of these parts. Based on Eq. (**7**), the long-range exchange interaction is described by the HF exchange integral,

$$E_x^{lr} = -\frac{1}{2}\sum_{\sigma}\sum_{i}^{occ}\sum_{j}^{occ}\iint \psi_{i\sigma}^{*}(\mathbf{r_1})\psi_{j\sigma}^{*}(\mathbf{r_2})\frac{erf(\mu r_{12})}{r_{12}}\psi_{j\sigma}(\mathbf{r_1})\psi_{i\sigma}(\mathbf{r_2})d^3\mathbf{r_1}d^3\mathbf{r_2}, \tag{8}$$

where $\psi_{i\sigma}$ is the *i*th σ-spin orthonormal molecular orbital. The LDA exchange functional is applied to the short-range exchange interaction such that

$$\begin{aligned} E_x^{sr} = &-\frac{3}{2}\left(\frac{3}{4\pi}\right)^{1/3}\sum_{\sigma}\int \rho_{\sigma}^{4/3}\left\{1-\frac{8}{3}a_{\sigma}\right. \\ &\left.\times\left[\sqrt{\pi}erf\left(\frac{1}{2a_{\sigma}}\right)+(2a_{\sigma}-4a_{\sigma}^3)\exp\left(-\frac{1}{4a_{\sigma}}\right)-3a_{\sigma}+4a_{\sigma}^3\right]\right\}d^3\mathbf{R}, \end{aligned} \tag{9}$$

where $a_{\sigma} = \mu/(2k_{\sigma})$. The averaged relative momentum k_{σ} is written for LDA as the Fermi momentum, *i.e.* $k_{F\sigma} = (6\pi^2\rho_{\sigma})^{1/3}$. Equation (**9**) is derived by using the density matrix form corresponding to the LDA exchange functional,

$$P_{1\sigma}^{LDA}\left(\mathbf{R}+\frac{\mathbf{r}}{2},\mathbf{R}-\frac{\mathbf{r}}{2}\right) = 3\frac{j_1(k_{F\sigma}r)}{k_{F\sigma}r}\rho_{\sigma}(\mathbf{R}), \tag{10}$$

where j_1 is the first-order spherical Bessel function.

However, Savin's scheme is inapplicable to conventional GGA exchange functionals, because

GGA functionals usually have no corresponding density matrices unlike LDA. In 2001, Iikura, Tsuneda, Yanai, and Hirao solved this problem by pushing gradient terms of GGA functionals into the momentum k_σ.[26] That is, the corresponding density matrix is determined for any GGA exchange functional by substituting $k_{F\sigma}$ in Eq. (**10**) with

$$k_\sigma^{GGA} = \left(\frac{9\pi}{K_\sigma^{GGA}} \right)^{1/2} \rho_\sigma^{1/3}, \tag{11}$$

where K_σ^{GGA} is defined in an exchange functional used: $E_x^{GGA} = \int \rho_\sigma^{4/3} K_\sigma^{GGA} d^3\mathbf{R}$. Equation (**11**) correctly reproduces the Fermi momentum $k_{F\sigma}$ for K_σ^{LDA}. By using k_σ^{GGA}, the short-range exchange energy in Eq. (**9**) is substituted by

$$E_x^{sr} = -\frac{3}{2}\left(\frac{3}{4\pi}\right)^{1/3} \sum_\sigma \int \rho_\sigma^{4/3} K_\sigma^{GGA} \left\{ 1 - \frac{8}{3} a_\sigma \right. \\ \left. \times \left[\sqrt{\pi}\, erf\left(\frac{1}{2a_\sigma}\right) + (2a_\sigma - 4a_\sigma^3) \exp\left(-\frac{1}{4a_\sigma}\right) - 3a_\sigma + 4a_\sigma^3 \right] \right\} d^3\mathbf{R}. \tag{12}$$

It is easily confirmed that Eq. (**12**) reproduces the original GGA exchange functional for μ=0. Parameter μ is determined to optimize bond distances of homonuclear diatomic molecules up to the third period as μ=0.33. This scheme is called ``long-range correction (LC) scheme''. The applicabilities of the LC scheme will be discussed in the later section.

Besides the LC scheme, we should mention the screened Coulomb potential hybrid functional as an attempt to take account of the long-range exchange effect. Heyd, Scuseria, and Ernzerhof developed this functional by dividing the exchange terms of the hybrid PBE0 functional into short- and long-range parts and by omitting a part of long-range exchange term as[27]

$$E_{xc}^{\omega PBEh} = aE_x^{HF,sr}(\omega) + (1-a)E_x^{PBE,sr}(\omega) + E_x^{PBE,lr}(\omega) + E_c^{PBE}, \tag{13}$$

where *a*=1/4 is a mixing coefficient and ω is an adjustable parameter. The main characteristics of this functional are the inclusion of the short-range HF exchange integral and the exclusion of the long-range HF exchange integral. This functional gives more accurate chemical properties than those of B3LYP for G2 and G3 set of molecules.[27,28] It is, however, presumed that this functional may not solve DFT problems arising from the lack of long-range exchange effects due to the exclusion of the long-range HF exchange integral. Moreover, Leininger, Stoll, Werner, and Savin extended the above Savin's scheme by using the long-range exchange integral for the multireference configuration interaction (MRCI) wavefunction.[29] Electron correlations in long-range interactions may hardly affect calculated properties of standard molecules. However, electron correlations may be important

for the comparison of molecules that have much different spin-multiplicity or neardegeneracy.

2.3. Applicabilities of long-range correction scheme

In this section, the LC scheme are examined by illustrating its applicabilities to three DFT problems that have never been solved: 1. poor reproducibilities of van der Waals bondings, 2. underestimations of Rydberg excitation energies, oscillator strengths, and charge transfer excitation energies in time-dependent density functional calculations, and 3. systematic overestimations of atomization energies of transition metal dimers.

2.3.1. Van der Waals calculations

One of the most critical DFT problems is the poor reproducibility of van der Waals (vdW) bondings. Actually, conventional correlation functionals have incorporated no vdW interactions. Since vdW bondings, however, often determine structures of large-scale molecules, accurate calculations of vdW bondings are a pressing problem in DFT. Several DFT studies have been made on vdW calculations by using, *e.g.*, a perturbation theory based on DFT.[30] The most effective and general way may be the use of a vdW functional. Up to the present, various types of vdW functionals have been suggested.[31,32,33] Some of these functionals reproduce accurate vdW C_6 coefficient comparable to the results of high-level *ab initio* methods.[31] However, these functionals give poor vdW bondings of, *e.g.*, rare gas dimmers by simply combining with a conventional exchange-correlation functional in DFT calculations. It is presumed that this problem may be due to the lack of long-range interactions in exchange functionals, because vdW bondings are supposed to be in the balance between vdW attraction and long-range exchange repulsion interactions. On this ground, Kamiya, Tsuneda, and Hirao applied the LC scheme with a vdW functional to calculations of dissociation potentials of rare-gas dimers.[34] Andersson-Langreth-Lundqvist (ALL) functional was used as the vdW functional.[31] This functional was developed to be correct for both separated electron gas regions and far-apart atoms. In this functional, a damping factor was used to diminish the vdW energy for regions at a short distance.

In Fig. 1, calculated dissociation potential energy curves of Ar_2 are shown for pure GGA functionals (BOP and PBEOP)[35] and LC functionals (LC-BOP and LC-PBEOP) with no vdW functionals. The 6-311++G(3df,3pd) basis functions was used.[36,37,38] The basis set superposition error was corrected by a counterpoise method.[39] As the figure shows, LC functionals give very close potential curves to each other, although pure GGA functionals provide obviously different curves. This may indicate that a long-range correction is necessary for exchange functionals to

reproduce vdW bondings.

Next, Figure 2 displays calculated dissociation potentials of Ar_2 by LC-BOP + ALL and conventional sophisticated functionals (mPWPW91,[40] mPW1PW91,[40] and B3LYP+vdW[41]). The 2nd-order Møller-Plesset perturbation (MP2) and experimentally-predicted (Expt.)[42] potential curves are also shown for comparison. The figure clearly shows that LC-BOP + ALL functional gives accurate vdW potential curve in comparison with the results of MP2 and other conventional DFTs. It is, therefore, necessary for accurate DFT calculations of vdW bondings to use both long-range-corrected exchange and vdw-incorporated correlation functionals.

2.3.2. Time-dependent density functional calculations

Time-dependent density functional theory (TDDFT) becomes widely-used as a simple method for rapid and accurate calculations of molecular excitation energies. It has, however, been reported that conventional TDDFT calculations underestimate Rydberg excitation energies, oscillator strengths, and charge-transfer excitation energies. Tawada, Tsuneda, Yanagisawa, Yanai, and Hirao supposed that this problem may also come from the lack of long-range exchange interaction, and applied the LC scheme to TDDFT calculations.[43]

Table 1 summarizes mean absolute errors in calculated excitation energies of five typical molecules by TDDFT. The table also displays calculated results of asymptotically-corrected AC[19] and LB[18] (AC-BOP and LBOP) and hybrid B3LYP[12] functionals, which are mentioned in the former section. The *ab initio* SAC-CI[44] results are also shown to confirm the accuracies. The 6-311G++(2d,2p) basis set was used in TDDFT calculations.[45,46] As the table indicates, the LC scheme clearly improves Rydberg excitation energies that are underestimated for pure BOP functional, at the same (or better) level as the AC scheme does. It should be noted that LC and AC schemes also provide improvements on valence excitation energies for all molecules. LC and AC results are comparable to SAC-CI results. The LB scheme clearly modifies Rydberg excitation energies, and however brings underestimations of valence excitation energies. B3LYP results are obviously worse than LC and AC results for both valence and Rydberg excitation energies.

Next, calculated oscillator strengths of excited states by TDDFT are shown in Table 2. As is clearly shown in the table, LC scheme drastically improves oscillator strengths, which are underestimated for BOP as second to hundredth part of experimental values, to the same digit. Although AC-BOP, LBOP, and B3LYP also provide closer oscillator strengths to the experimental values than BOP do, the accuracies are unsatisfactory in comparison with LC-BOP ones. It is, therefore, concluded that the lack of long-range interactions in exchange functional may also cause the underestimations of oscillator strengths in TDDFT calculations.

Finally, calculated lowest charge transfer excitation energies of ethylene-tetrafluoroethylene dimer

are shown in Fig. 3. Dreuw et al. recently suggested that poor charge transfer excitation energies of far-aparted molecules may be one of the main problems of TDDFT.[47] They pointed out that intermolecular charge transfer excitation energies of far-aparted molecules should have the correct asymptotic behavior for long intermolecular distance. That is, for long molecular-molecular distances R and R_0 ($R > R_0$), charge transfer energy ω_{CT} should satisfy

$$\omega_{CT}(R) - \omega_{CT}(R_0) \geq -\frac{1}{R} + \frac{1}{R_0}. \qquad (\mathbf{14})$$

The figure shows that LC-BOP gives the correct asymptotic behavior as is different from AC-BOP and LBOP do. Although B3LYP recovers a part of this behavior, the degree is in proportion to the mixing rate of the HF exchange integral. Hence, this result may also indicate that problems in conventional TDDFT calculations come from the lack of long-range exchange interactions in exchange functionals rather than the poor far-nucleus asymptotic behavior of exchange functionals.

2.3.3. Transition metal dimer calculations

Yanagisawa, Tsuneda, and Hirao calculated the equilibrium geometries and the atomization energies for the first- to third-row transition metal dimers and concluded that[48,49]

1. Pure functionals tend to overstabilize electron configurations that contain orbitals in a high angular momentum shell that is not fully occupied. This tendency is reduced from the first- to third-row transition metal dimers.
2. The overestimations of atomization energies of dimers are associated with the errors in outermost *s*-*d* interconfiguration transition energies of atoms. The latter errors may be due to the lack of long-range exchange interactions of outermost *s* and *d* orbitals that are fairly different in distributions. Hence, this lack may also cause the overestimations of the atomization energies.
3. B3LYP generally gives more accurate atomization energies than those of pure functionals, even if high angular momentum orbitals are present in the configuration. However, B3LYP gives an erroneous energy gap between the configurations of fairly different spin-multiplicity probably due to the unbalance of the exchange and correlation functionals.

Based on this discussion, Tsuneda, Tokura, and Hirao applied the LC scheme to calculations of transition metal dimers.[50]

Errors in calculated atomization energies of transition metal dimers are displayed in Fig. 4. The Wachters + f basis set was used.[51,52,53] The figure shows that the LC scheme obviously improves the systematic overestimations calculated by pure BOP functional. It was, therefore, proved that these overestimations may be due to the lack of long-range exchange interactions in exchange functionals. It was also found that LC-BOP fairly underestimates the atomization energies of V_2 and Cr_2. As supposed from the similarity to B3LYP results, this underestimation may come from the

errors in the HF exchange integral. That is, the HF exchange integral overstabilizes high-spin electronic states, because it only incorporates parallel-spin electron-electron interactions. It is, therefore, expected that this problem may be solved by taking well-balanced electron correlation into account for the long-range exchange part. The figure also shows that the LC scheme makes calculated atomization energies of different functionals much closer to each other. That is, the uniquenesses of functionals dissappeared after the long-range correction in this calculation. This may also support the conclusion that the lack of long-range exchange interactions is deeply-committed to the overestimated atomization energies of dimers.

2.3.4. Other calculations

Besides the above-mentioned calculations, Tsuneda *et al.* are now applying the LC scheme to calculations of chemical reactions[54] and (hyper)polarizabilities.[55] We will exhibit some present works to show the wide applicabilities of this scheme.

First, calculated results of $H_2 + H \rightarrow H + H_2$ reaction are summarized in Table 3.[54] The pV6Z basis set was used.[56] The table shows that the LC scheme remarkably improves underestimated reaction barrier energies of BOP. As far as we know, this result is certainly superior to results of other corrections that have ever reported. This may indicate that underestimations of reaction barriers in DFT calculations are also due to the lack of long-range interactions.

The LC scheme was also applied to overestimations of polarizabilities in DFT as shown in Table 4.[55] The Sadlej valence triple zeta basis set was used.[57,58] The table shows that calculated polarizabilities of LC-BOP are obviously more accurate than those of BOP. Compared to B3LYP results, LC-BOP shows more improvements in many cases. Similar results were found in calculations of anisotropies and S_{-4} Causchy moments of polarizabilities. Hence, we may say that these overestimations also come from the lack of long-range interactions in exchange functionals.

As mentioned above, the LC scheme was found to give better results for various chemical properties than the results of conventional corrections including hybrid functionals. For some properties, the LC scheme provided equivalent improvements in comparison with B3LYP. This may indicate that accurate B3LYP results may be due to the equivalency in the mixed HF exchange energy to the LC scheme, rather than the validity of the constant weight hybridization of the HF exchange. This argument may require further examination of the LC scheme.

Figure captions

Fig. 1. Calculated bond energy potentials of argon dimer for long-range exchange corrected functionals (LC-SOP, LC-BOP, and LC-PBEOP). Pure functionals are also presented for comparison. Highly accurate potentials are also shown for comparison.

Fig. 2. Calculated bond energy potentials of argon dimer for LC-BOP+ALL functional. For comparison, calculated potentials of conventional sophisticated density functional schemes (mPWPW91, mPW1PW91, and B3LYP+vdW) and those of MP2 are also presented. Highly accurate potentials are also shown for comparison.

Fig. 3. The lowest charge transfer excitation energy of ethylene-tetrafluoroethylene dimer for the long intermolecular distance calculated by TDDFT employing various types of functionals. For all methods, the excitation energy at 5.0 Å is set to zero.

Fig. 4. Errors in calculated atomization energies of the first-row transition metal dimers for LC functionals (LC-BOP and LC-PBEOP), pure functionals (BOP and PBEOP), and B3LYP in eV. The line of no-error is also illustrated.

Tables

Table 1. Mean absolute errors in calculated excitation energies of five typical molecules by TDDFT in eV.

Molecule		LC-BOP	BOP	AC-BOP	LBOP	B3LYP	SAC-CI
N_2	Valence	0.36	0.40	0.27	1.48	0.54	0.33
	Rydberg	0.90	2.37	0.84	0.43	1.30	0.25
	Total	0.54	1.06	0.46	1.13	0.79	0.30
CO	Valence	0.19	0.28	0.17	1.02	0.36	0.26
	Rydberg	0.75	2.06	0.79	0.42	1.16	0.27
	Total	0.47	1.17	0.48	0.72	0.76	0.27
H_2CO	Valence	0.25	0.59	0.24	0.52	0.26	0.45
	Rydberg	0.47	1.66	0.59	0.07	0.84	0.13
	Total	0.40	1.30	0.47	0.22	0.64	0.24
C_2H_4	Valence	0.30	0.47	0.24	1.52	0.47	0.11
	Rydberg	0.18	1.41	0.58	0.69	0.92	0.17
	Total	0.20	1.28	0.53	0.80	0.85	0.16
C_6H_6	Valence	0.21	0.28	0.24	0.84	0.26	0.35
	Rydberg	0.24	1.01	0.88	0.35	0.56	0.15
	Total	0.23	0.74	0.64	0.53	0.44	0.22

Table 2. Calculated oscillator strengths of excited states of typical molecules by TDDFT ($x10^{-2}$).

System	State	LC-BOP	BOP	AC-BOP	LBOP	B3LYP	SAC-CI	Exp.
N_2	$^1\Pi_u$	11.05	0.28	2.02	4.18	1.33	8.14	24.3
	$^1\Sigma_u^+$	24.06	0.69	6.07	3.60	3.84	15.67	27.9
CO	$^1\Pi$	19.76	8.66	6.68	5.97	11.24	9.63	17.6
H_2CO	$^1B_2$	2.19	1.68	1.02	3.02	2.71	1.88	4.13,2.8,3.8,3.2
	$^1A_1$	6.94	2.11	2.62	1.80	3.64	4.26	6.05,3.2,3.8,3.6
	$^1B_2$	6.50	1.75	2.42	2.23	2.32	2.95	2.81,1.7,1.9
C_2H_4	$^1B_{3u}$	12.85	3.49	4.77	5.08	6.75	8.20	4.00
	$^1B_{1u}$	73.85	12.85	24.41	32.38	34.67	40.65	29.00
C_6H_6	1^1E_{1u}	134.02	49.71	48.59	53.48	58.31	103.05	120,90.0,95.3

Table 3. Calculated barrier energies and bond distances of $H_2 + H \rightarrow H + H_2$ reaction. Barrier energies are in kcal/mol and optimized geometries are in Å. Reference values (Refs.) are the quantum Monte Carlo results.

Molecule	Barrier height		Optimized geometry	
Functional	Classical	ZPVC	$R(H_2)$	$R(H_3)$
LC-BOP	10.1	9.3	0.752	0.940
BOP	3.5	2.8	0.743	0.934
BLYP	2.9	2.2	0.745	0.930
B3LYP	4.3	3.5	0.742	0.934
Refs.	---	9.6	0.741	---

Table 4. Calculated static isotropic polarizabilities by time-dependent Kohn-Sham theory in atomic unit.

Molecule	LC-BOP	BOP	B3LYP	Exp.
Cl_2	30.87	31.69	31.16	30.35
CO_2	17.58	17.82	17.36	17.51
F_2	8.83	8.87	8.69	8.38
H_2O	10.03	10.49	9.95	9.64
H_2S	24.72	25.64	25.11	24.71
HCl	17.74	18.33	17.90	17.39
HF	5.99	6.17	5.83	5.60
N_2	11.99	12.07	11.88	11.74
SO_2	25.63	26.30	25.75	25.61

Figures

Fig. 1

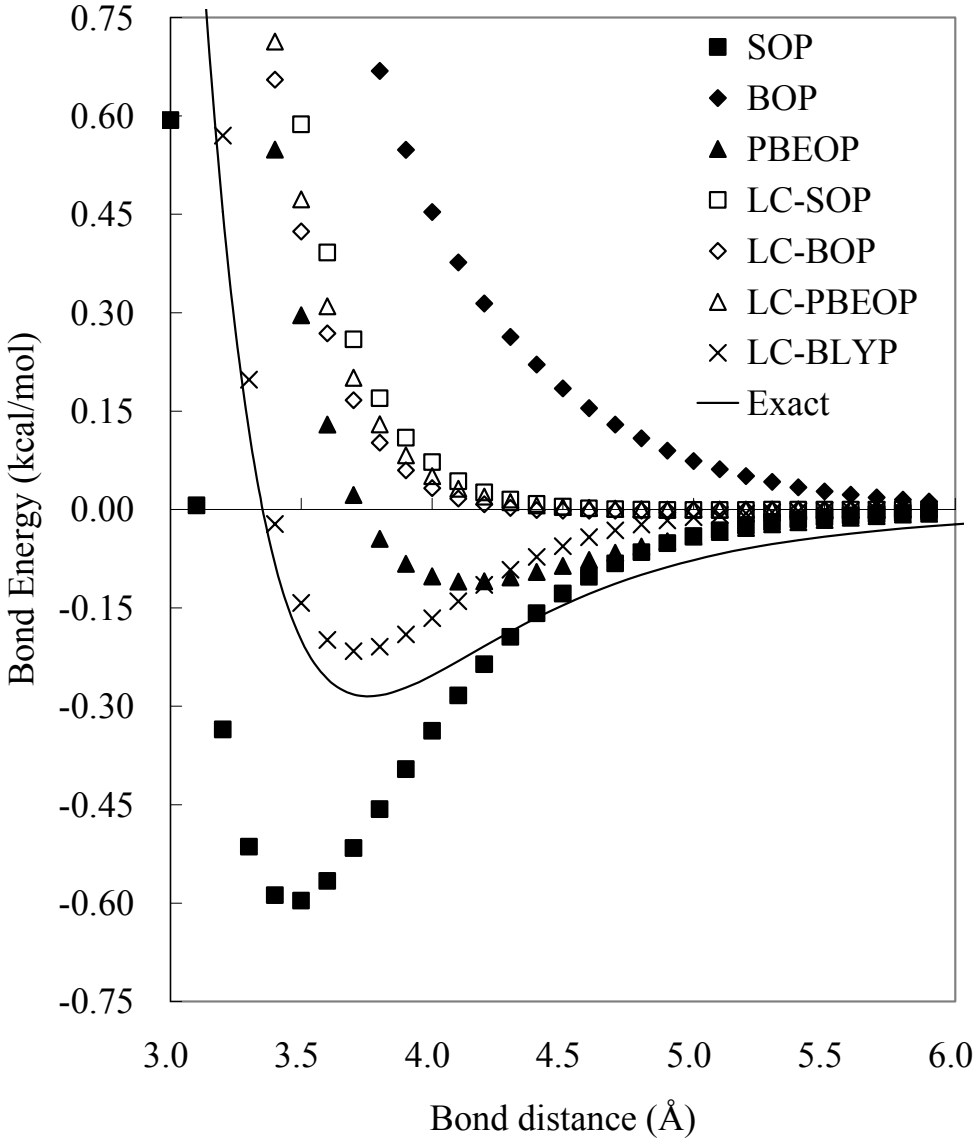

Fig. 2

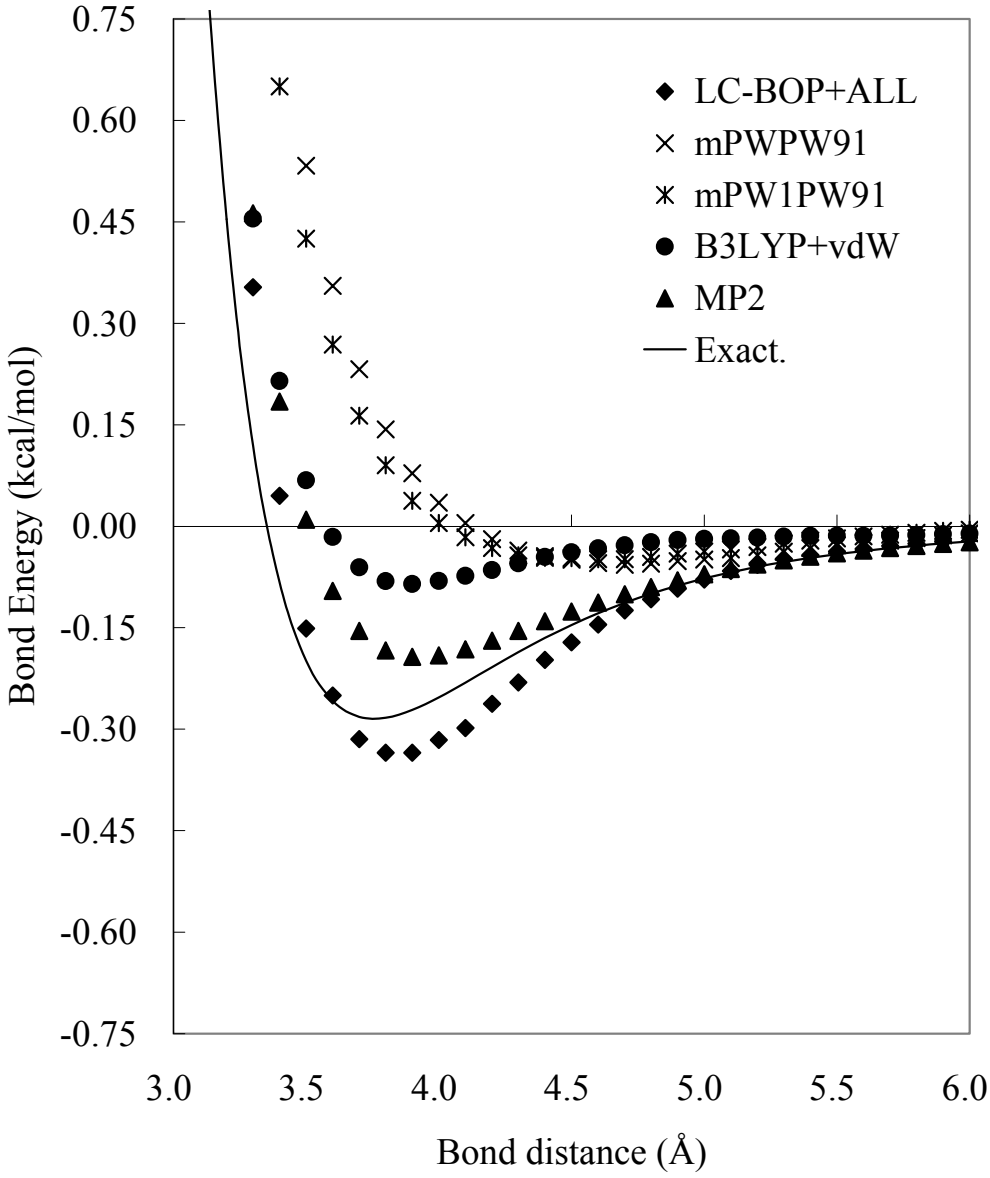
0.75
0.60
0.45
0.30
0.15
0.00
-0.15
-0.30
-0.45
-0.60
-0.75
Bond Energy (kcal/mol)
3.0
3.5
4.0
4.5
5.0
5.5
6.0
Bond distance (Å)
LC-BOP+ALL
mPWPW91
mPW1PW91
B3LYP+vdW
MP2
Exact.

Fig. 3

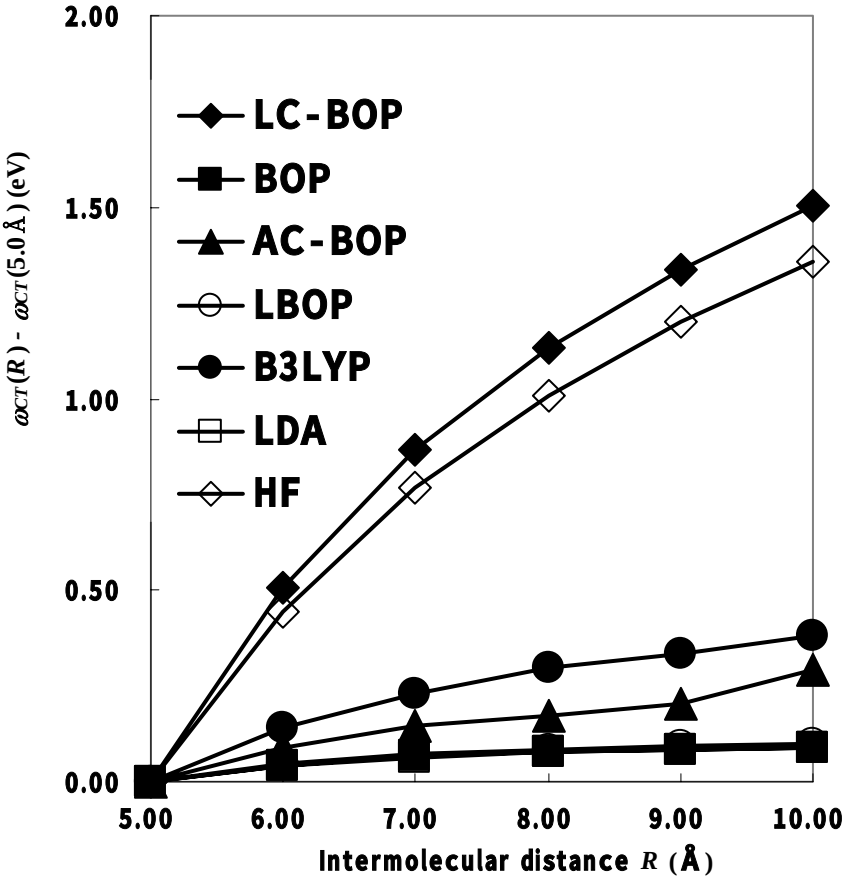
2.00
1.50
1.00
0.50
0.00
5.00
6.00
7.00
8.00
9.00
10.00
LC-BOP
BOP
AC-BOP
LBOP
B3LYP
LDA
HF
ωCT(R) - ωCT(5.0 Å) (eV)
Intermolecular distance R (Å)

Fig. 4

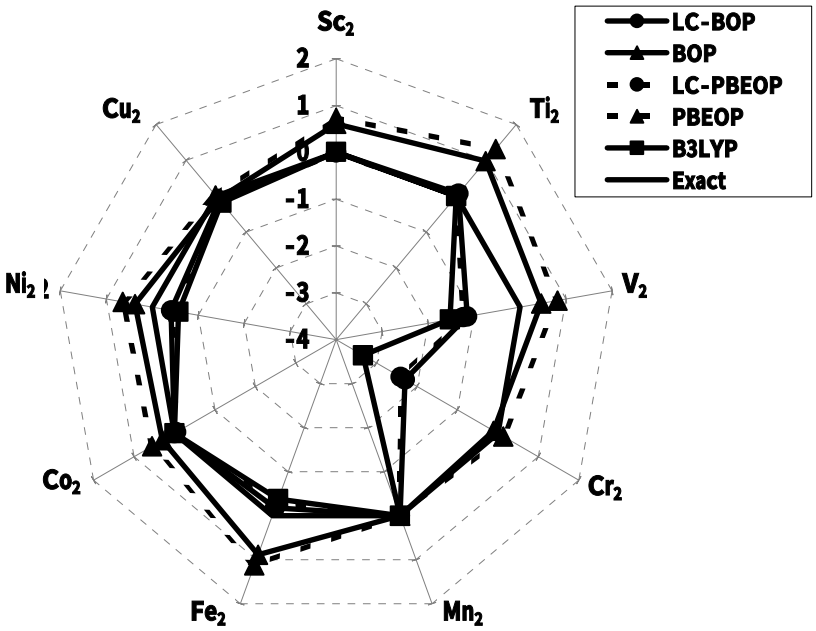
Sc2
Ti2
V2
Cr2
Mn2
Fe2
Co2
Ni2
Cu2
2
1
0
-1
-2
-3
-4
LC-BOP
BOP
LC-PBEOP
PBEOP
B3LYP
Exact

References

1 W. Kohn and L. J. Sham, Phys. Rev. A 140, 1133 (1965).

2 R. G. Parr and W. Yang, *Density-Functional Theory of Atoms and Molecules* (Oxford University Press, New York, 1989).

3 R. M. Dreizler and E. K. U. Gross, *Density-Functional Theory: An Approach to the Quantum Many-Body Problem* (Springer-Verlag, Berlin Heidelberg, 1990).

4 A. D. Becke, Phys. Rev. A 38, 3098 (1988).

5 J. P. Perdew and Y. Wang, in *Electronic Strucure of Solids '91*, Eds. P. Ziesche and H. Eschrig (Akademie Verlag, Berlin, 1991).

6 J. P. Perdew, K. Burke and M. Ernzerhof, Phy. Rev. Lett. 77, 3865 (1996).

7 T. Tsuneda and K. Hirao, Phys. Rev. B 62, 15527 (2000).

8 J. C. Slater, Phys. Rev. 81, 385 (1951).

9 T. Tsuneda, T. Suzumura and K. Hirao, J. Chem. Phys. 111, 5656 (1999).

10 T. Tsuneda, M. Kamiya, N. Morinaga and K. Hirao, J. Chem. Phys., 114, 6505 (2001).

11 L. Kleinman and S. Lee, Phys. Rev. B 37, 4634 (1988).

12 A. D. Becke, J. Chem. Phys. 98, 5648 (1993).

13 C. Lee, W. Yang and R. G. Parr, Phys. Rev. B 37, 785 (1988).

14 S. H. Vosko, L. Wilk and M. Nusair, Can. J. Phys. 58, 1200 (1980).

15 A. D. Becke, J. Chem. Phys. 107, 8554 (1997).

16 J. P. Perdew, K. Burke and M. Ernzerhof, J. Chem. Phys. 105, 9982 (1996).

17 M. Levy, J. P. Perdew and V. Sahni, Phys. Rev. A 30, 2745 (1984).

18 R. van Leeuwen and E. J. Baerends, Phys. Rev. A 49, 2421 (1994).

19 D. J. Tozer and N. C. Handy, J. Chem. Phys., 109, 10180 (1998).

20 D. J. Tozer, J. Chem. Phys., 112, 3507 (1999).

21 J. P. Perdew and A. Zunger, Phys. Rev. B, 23, 5048 (1981).

22 B. G. Johnson, C.A . Gonzales, P. M. W. Gill and J. A. Pople, Chem. Phys. Lett. 221, 100 (1994).

23 X. Tong and S. Chu, Phys. Rev. A 55, 3406 (1997).

24 T. Tsuneda, M. Kamiya and K. Hirao, J. Comput. Chem., 24, 1592 (2003).

25 A. Savin, in *Recent Developments and Applications of Modern Density Functional Theory*, Ed. J. M. Seminario (Elsevier, Amsterdam, 1996), p. 327.

26 H. Iikura, T. Tsuneda, T. Yanai and K. Hirao, J. Chem. Phys. 115, 3540 (2001).

27 J. Heyd, G. E. Scuseria and M. Ernzerhof, J. Chem. Phys. 118, 8207 (2003).

28 J. Heyd and G. E. Scuseria, J. Chem. Phys. 120, 7274 (2004).

29 T. Leininger, H. Stoll, H.-J. Werner, and A. Savin, Chem. Phys. Lett. 275, 151 (1997).

30 H. L. Williams and C. F. Chabalowski, J. Phys. Chem· 105, 646 (2001).

31 Y. Andersson, D. C. Langreth and B. I. Lundqvist, Phys. Rev. Lett. 76, 102 (1996).

32 K. Rapcewicz and N. W. Ashcroft, Phys. Rev. B 44, 4032 (1991).

33 W. Kohn, Y. Meier and D. E. Makarov, Phys. Rev. Lett. 80, 4153 (1998).

34 M. Kamiya, T. Tsuneda, and K. Hirao, J. Chem. Phys. 117, 6010 (2002).

35 T. Tsuneda, T. Suzumura and K. Hirao, J. Chem. Phys. 110, 10664 (1999).

36 R. Krishnan, J. S. Binkley, R. Seeger and J.A. Pople, J. Chem. Phys. 72, 650 (1980).

37 A. D. McLean and G. S. Chandler, J. Chem. Phys. 72, 5639 (1980).

38 M. J. Frisch, J. A. Pople and J. S. Binkley, J. Chem. Phys. 80, 3265 (1984).

39 S. F. Boys and F. Bernardi, Mol. Phys. 19, 553 (1970).

40 C. Adamo and V. Barone, J. Chem. Phys. 118, 664 (1998).

41 Q. Wu and W. Yang, J. Chem. Phys. 116, 515 (2002).

42 J. F. Oglivie and F. Y. H. Wang, J. Mol. Struct. 273, 277 (1992).

43 Y. Tawada, T. Tsuneda, S. Yanagisawa, T. Yanai and K. Hirao, J. Chem. Phys. 120, 8425 (2004).

44 H. Nakatsuji, Chem. Phys. Lett., 59, 362 (1978).

45 R. Krishnan, J. S. Binkley, R. Seeger, and J. A. Pople, J. Chem. Phys., 72, 650 (1980).

46 A. D. McLean and G. S. Chandler, J. Chem. Phys., 72, 5639 (1980).

47 A. Dreuw, J. L. Weisman, and M. Head-Gordon, J. Chem. Phys., 119, 2943 (2003).

48 S. Yanagisawa, T. Tsuneda and K. Hirao, J. Chem. Phys., 112, 545 (2000).

49 S. Yanagisawa, T. Tsuneda and K. Hirao, J. Comput. Chem., 22, 1995 (2001).

50 T. Tsuneda, S. Tokura, and K. Hirao, in preparation.

51 A. J. H. Wachters, J. Chem. Phys. 52, 1033, 1970.

52 A. J. H. Wachters, IBM Tech. Rept. RJ584, 1969.

53 C. W. Bauschlicher, Jr. S. R. Langhoff and L. A. Barnes, J. Chem. Phys. 91, 2399, 1989.

54 T. Tsuneda, N. Kawakami, and K. Hirao, in preparation.

55 M. Kamiya, T. Tsuneda, and K. Hirao, in preparation.

56 T. H. Dunning Jr, to be published.

57 A. J. Sadlej, Theor. Chim. Acta, 81, 339 (1992).

58 M. E. Casida, C. Jamorski, K. C. Casida, and D. R. Salahub, J. Chem. Phys., 108, 4439 (1998).